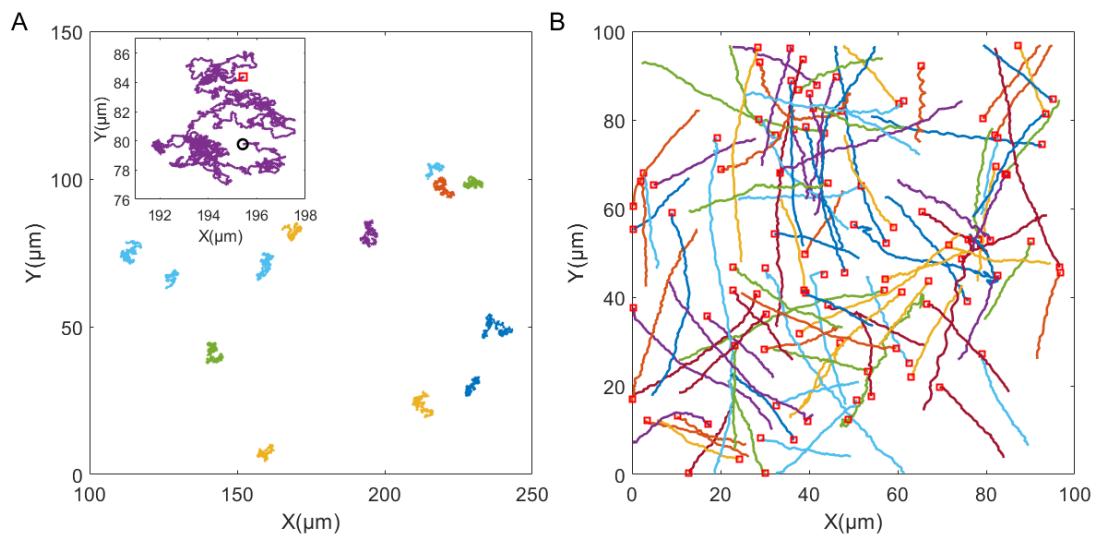


## Supporting Information

**Table. S1.** Cell length and swimming speed of bacterial strains used in this work

Strains	Cell length (μm)	Swimming speed (μm/s) <sup>a</sup>
PAO1 $\Delta$ pilA	3.5 ± 1.3	27.5 ± 1.8 (n = 22)
PAO1 $\Delta$ pilA + NaN3	3.3 ± 1.3	21.6 ± 1.3 (n = 11)
HCB1284- <i>fliC</i>	3.6±1.4	15.9 ± 2.4 (n = 11)
HCB1284- <i>fliC</i> + Serine	3.6±1.4	20.9 ± 1.3 (n = 19)
HCB1284- <i>fliC</i> + Serine + NaN3	3.5±1.4	14.4 ± 1.2 (n = 11)
HCB33- <i>fliC</i>	3.5±1.3	15.3 ± 1.8 (n = 22)

<sup>a</sup> Values are mean ± standard deviation of sample velocities; n = number of samples, each sample comprising >100 measured cells.



**Fig. S1.** Example trajectories of tracer beads and swimming cells. (A) Trajectories of 3.0  $\mu\text{m}$  beads lasting longer than 30 s, recorded at 33.3 frames per second. Inset: an example of an individual bead's loopy trajectory, with the red square and black circle indicating the start and end points, respectively. (B) Trajectories of swimming bacteria tracked over more than 20 frames, with the red square marking the starting position.

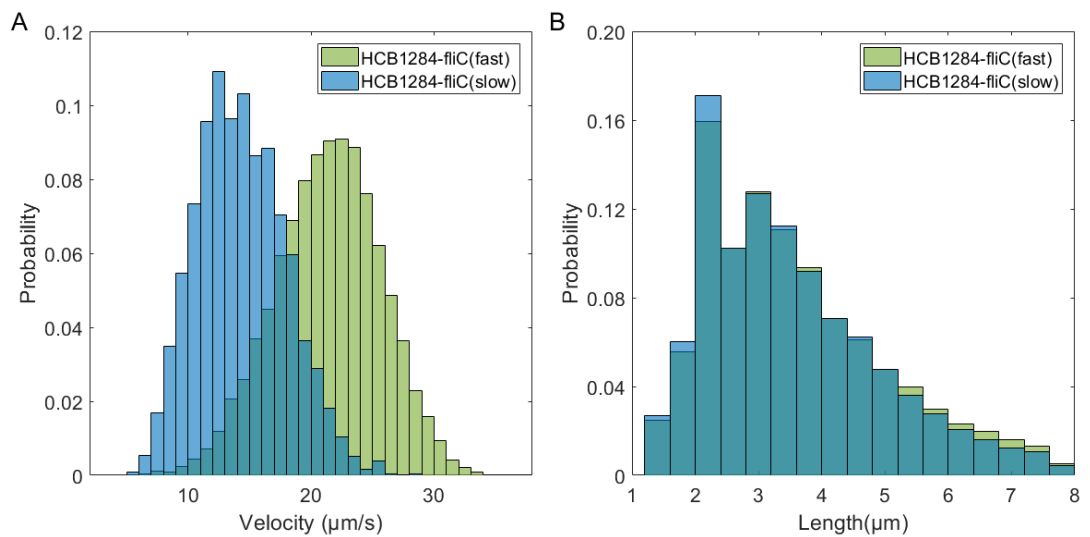


**Fig. S2.** Distributions of bacterial swimming speed and cell length. (A) Distribution of swimming speeds for HCB1284-fliC bacteria. The fast population (green bars) peaks at  $\sim 20.9 \pm 1.3 \mu\text{m/s}$ , while the slow population (blue bars) peaks at  $\sim 14.4 \pm 1.2 \mu\text{m/s}$ . Errors represent standard deviation of sample velocities (Table S1). (B) Probability distribution of bacterial cell lengths. The average length for the fast population is  $\sim 3.6 \pm 1.4 \mu\text{m}$  (mean  $\pm$  standard deviation), and for the slow population is  $\sim 3.5 \pm 1.4 \mu\text{m}$  (mean  $\pm$  standard deviation).

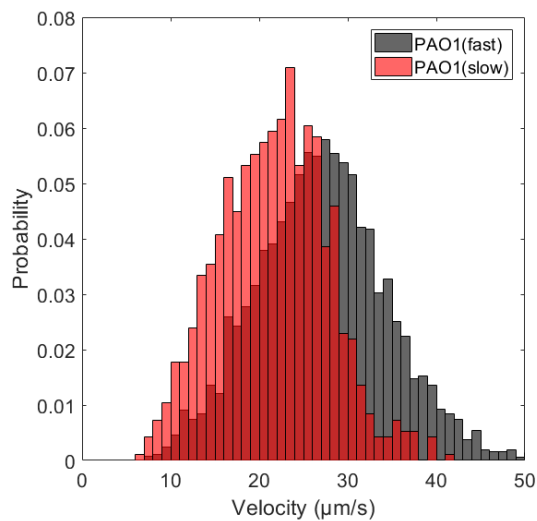


**Fig. S3.** Distribution of bacterial swimming speeds in PAO1 suspensions. The speed distribution for PAO1 bacteria exhibits peaks at  $\sim 27.5 \pm 1.8 \mu\text{m/s}$  for the fast population (black bars) and  $\sim 21.6 \pm 1.3 \mu\text{m/s}$  for the slow population (red bars).

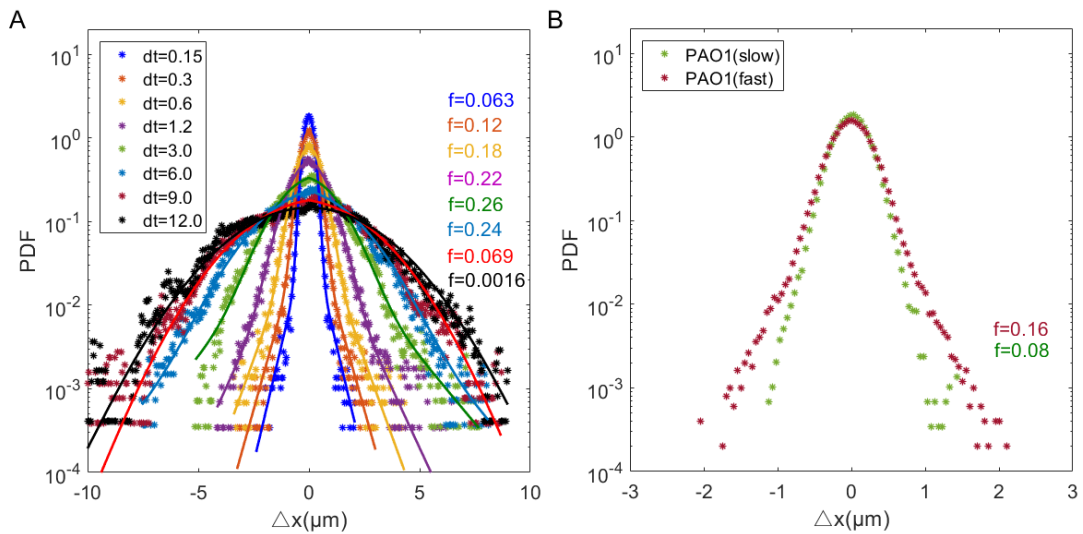


**Fig. S4.** Probability distribution functions (PDFs) of microsphere displacements. (A) Experimental PDFs of microsphere displacements ( $\Delta x$ ) measured over various time intervals ( $dt$ ). The distributions feature a Gaussian core and an exponential tail. The fraction ( $f$ ) of the exponential component first increases and then decreases as  $dt$  increases. Different colors represent the fitting curves corresponding to the respective  $f$  values, where a larger  $f$  value indicates a greater proportion of the exponential tail in the distribution. (B) Probability density function of microsphere displacements for PAO1 fast (red) and slow (green) populations at the same bacterial density, measured over a 0.15 s interval. The fast PAO1 population exhibits a higher exponential tail fraction ( $f=0.16$ ) compared to the slow population ( $f=0.08$ ).

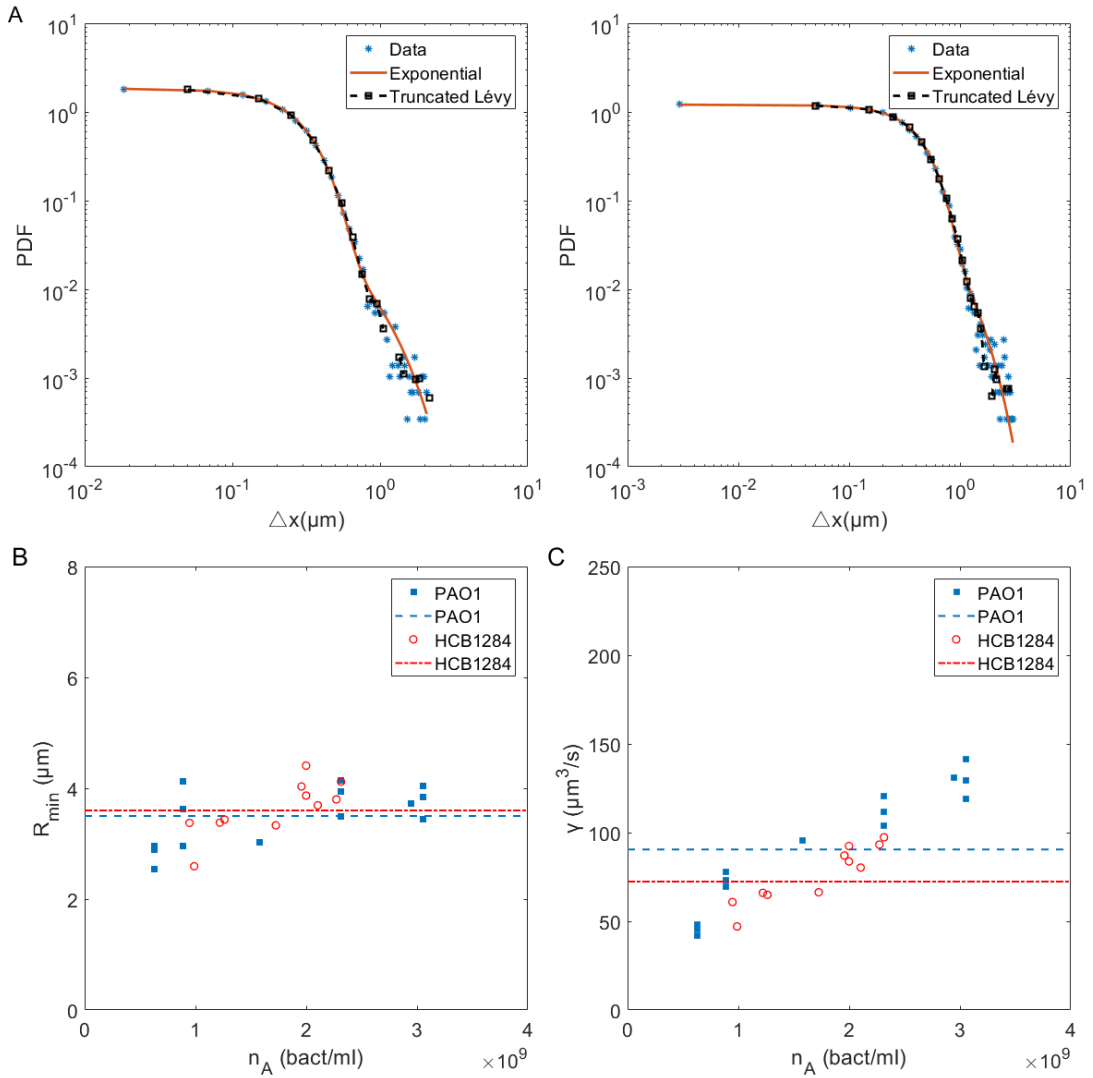


**Fig. S5.** Comparison of different fitting models. (A) Two examples of the displacement distribution  $P(dx, dt)$  of PAO1 from Fig. S4. Blue points represent the experimental data. The characterizations of two models are shown: orange lines represent a superposition of Gaussian and exponential distributions; black dashed lines are fits of the inverse Fourier transform of displacement function from the truncated Lévy model. All models agree well with the experimental data. (B and C) Fit values for  $R_{\min}$  and  $\gamma$  from the truncated Lévy model. Blue and red dashed lines indicate the averages for PAO1 and HCB1284, respectively.

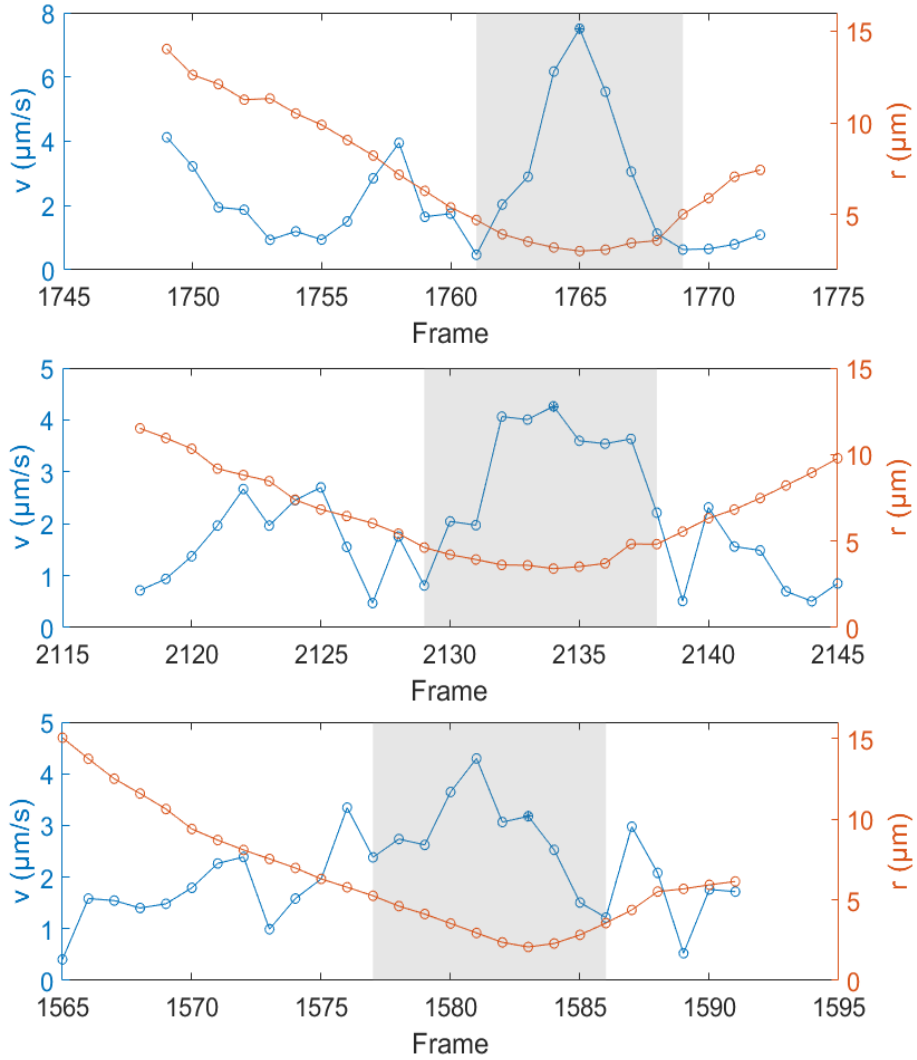


**Fig. S6.** Representative time traces of individual bacterium-tracer interactions. Time-series data showing the tracer particle's speed ( $v$ , blue curve, left y-axis) and the bacterium-tracer distance ( $r$ , orange curve, right y-axis). The shaded regions highlight periods of 9-10 frames centered on the maximum tracer speed, which nearly coincide with periods where the bacterium is within the effective interaction radius. These intervals of close proximity directly correspond to significant enhancements in the tracer's speed, elevating it above the baseline level of Brownian motion. Three representative examples are shown, each demonstrating the clear correlation between proximity and speed enhancement. This provides independent corroboration for the interaction radius estimated in Fig. 4.

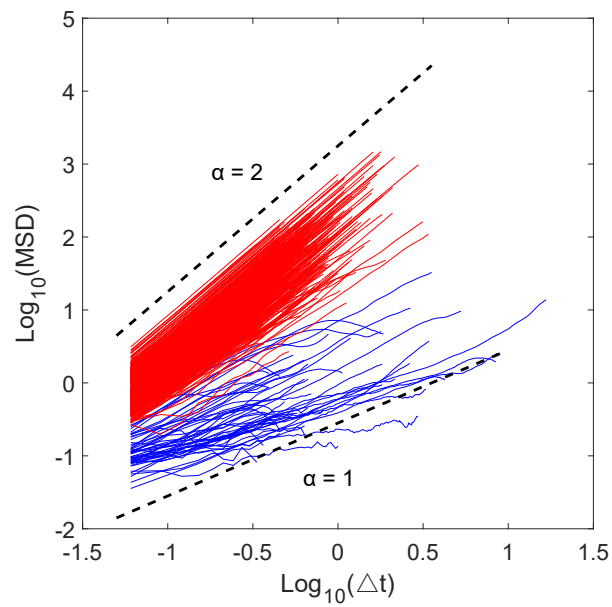


**Fig. S7.** Examples of MSD for motile (red lines) and non-motile (blue lines) bacteria. The  $\alpha$  values of non-motile bacteria are below 1.2. The black dashed lines represent the reference lines for  $\alpha = 1$  and  $\alpha = 2$ , respectively.